OPEN ACCESS Int. J. Phytopathol. 08 (02) 2019. 37-51 DOI: 10.33687/phytopath.008.02.2943

Available Online at EScience Press
International Journal of Phytopathology
ISSN: 2312-9344 (Online), 2313-1241 (Print)
https://esciencepress.net/journals/phytopath

MOLECULAR AND PATHOLOGICAL VARIABILITY ASSOCIATED WITH TRANSPOSABLE ELEMENTS OF *BOTRYTIS CINEREA* ISOLATES INFECTING GRAPE AND STRAWBERRY IN EGYPT

[a]Elsayed E. Wagih, [b]Hala Abdel Wahab*, [a]Mohamed. R. A. Shehata, [a]Magda. M. Fahmy, [a]Mahmoud. A. Gaber
[a] Department of Plant Pathology, College of Agriculture, El-Shatby, University of Alexandria, Alexandria, Egypt.
[b] Laboratory of Molecular Diagnostic of Plant Diseases, Department of Plant Pathology, Faculty of Agriculture, Ain Shams University, Cairo, Egypt.

**Corresponding Author Email: hala_abdelwahab@agr.asu.edu.eg*

A B S T R A C T

Grey mold caused by *Botrytis cinerea*, is known to cause great losses in most vegetable and fruit crops. Fifty-one isolates of *B. cinerea* were collected from grape (BCG) and strawberry (BCS) grown in different Egyptian locations. Variation among isolates was demonstrated using fenhexamid resistance and genetic approaches. Isolates were classified into various pathogenic groups depending on their reactions towards lettuce leaves. Genetic variability was identified in all isolates using transposable elements (TEs) analysis which revealed either the presence or absence of *boty* and *flipper* transposons. Furthermore, TEs typing of *B. cinerea* isolates demonstrated four TE types, on the basis of TE distribution in *B. cinerea* populations, namely, *transposa* (having both boty and flipper), *flipper* (possessing only *flipper*), *boty* (having only *boty*), and *vacuma* (lacking both *boty* and *flipper* elements). *Transposa* type was predominant (43.1%) and both *transposa* and *vacuma* isolate types showed no specialization with respect to host plant or plant location, while *flipper* type revealed a geographical preference in (BCG) isolates. Pathogenicity was also correlated to TE type as isolates containing *transposa* type revealed some degree of correlation with virulence behaviour, suggesting that *transposa* populations have higher pathogenic potential as compared to *vacuma* ones. The sensitivity of sampled isolates was tested against fenhexamid as one of the most important botryticides. Sensitivity to fenhexamid was shown in all isolates from strawberry and grape, grown in different locations, with low EC50 values between 0.012-0.084 µg/ml. This finding provided a cue for effective usage of fenhexamid for grey mold management. The present work demonstrated a correlation between the distribution of TEs and some fungal features such as isolate source and virulence, but no correlation was found between morphological characteristics, TE type, and sensitivity to fenhexamid. Cluster analysis based on phylogenetic tree showed that the Egyptian isolates branched as a separate divergent group from the others retrieved from GenBank, reflecting the presence of sequence polymorphism between the current isolates of *B. cinerea* and those previously identified.

Keywords: Grey mold, Fungicide sensitivity, Transposable elements, Phylogenetic divergence.

INTRODUCTION

Botrytis cinerea sensu lato, the causal agent of grey mold disease, is a phytopathogenic necrotrophic fungus. It causes extensive pre- and post-harvest damages and infects over 200 plant species worldwide. *B. cinerea* is not host specific and shows virulence variation towards different host plants (Mirzaei *et al.*, 2009). This fungus is a complex pathogen due to its high flexibility in adapting to various host plants and environmental conditions.

Typical symptoms comprising of greyish soft rotten of infected plant part lead to great production loss in affected plants in a broad spectrum of hosts. Morphological characteristics such as fungal mycelia, conidia and sclerotia are useful features in the study of *B. cinerea* isolates. Generally, variability in fungi is manifested in morphology (Chardonnet *et al.*, 2000), pathogenicity (Wahab *et al.*, 2019), fungicide resistance (Abdel Wahab, 2015) and genomic instability (Dufresne *et al.*, 2006; LÓPez-Berges *et al.*, 2009) including ploidy (Buttner *et al.*, 1994). Genetic variation of fungal pathogen had been detected using

molecular techniques such as genomic transposable elements (Dufresne *et al.*, 2006; LÓPez-Berges *et al.*, 2009; Abdel Wahab, 2015) restriction fragment length polymorphism (Giraud *et al.*, 1997), DNA fingerprinting repetitive sequences (Ma and Michailides, 2005), amplified fragment length polymorphism (Moyano *et al.*, 2003) and genomic typing by microsatellite (Fournier *et al.*, 2002). These methods had made a significant impact on fungal identification, taxonomic and phylogenetic studies (Fournier *et al.*, 2005). More noticeably, the development of specific primers against *B. cinerea* genomic has permitted fast detection at the genus/species levels (Karakaya and Bayraktar, 2009).

Although many studies have been conducted, a regular trend and a positive correlation between biological and ecological features are still in need to be established (Mirzaei *et al.*, 2009). Because of the genetic plasticity of *B. cinerea*, a high evolutionary potential of resistant strains makes fungicides to be hardly adopted by farmers in order to totally eradicate grey mold disease. The potential of some fungicides had been evaluated on the basis of the phenotypic and genetic diversity among fungal strains (Ahmed and Naim, 1993; Tanovic *et al.*, 2009). However, more evaluations are needed to be studied as these fungicides are always affected by environmental factors. Thus, the purposes of the current study were to (i) discriminate *B. cinerea* isolates collected from different locations in Egypt on the basis of their morphological, pathogenic, and molecular features; (ii) combine such data to generate a robust characterization of *B. cinerea* isolates; (iii) establish the phylogenetic relationships among *B. cinerea* isolates with respect to geographic origin and host plants; and (iv) test sensitivity of *B. cinerea* isolates towards fenhexamid which is effectively used for the control of this fungus.

MATERIALS AND METHODS

Collection of plant samples: Plant samples were collected from symptomatic and asymptomatic berries of grape (*Vitis vinifera*) and fruits of strawberry (*Fragaria ananassa*), grown in five Egyptian locations during 2015-2016 (Table 1).

Table 1. Collection of *Botrytis cinerea* from naturally diseased grapes and strawberry.

Host plant	Plant organ	District	Isolate code	No. isolates
Strawberry	Fruits	EL-Beheira (Badr)	BCS101 - BCS110	26
		EL-Beheira (Kom Hamada)	BCS111 - BCS122	
		El-Sharqia	BCS123 - BCS126	
Grape	Berries	Matruh	BCG101 - BCG105	25
		EL-Beheira	BCG106 - BCG115	
		Alexandria	BCG116 - BCG125	

Collection and phenotypic characteristics of *Botrytis cinerea* isolates: In order to isolate *B. cinerea* from symptomatic and asymptomatic plants, modified selective medium (m1KERS) was prepared according to Abdel Wahab and Helal (2013). Samples were cut into small pieces (0.5cm), put in sterilized water for 5 min, dried on sterilized filter paper, then put on m1KERS medium and incubated for 3-21 days at 23 °C. A pure culture was obtained by the monospore technique using potato dextrose agar (PDA) medium. Single spore cultures were preserved using sterilized paraffin oil at 4°C. Cultural and morphological characteristics of *B. cinerea* isolates were described according to Ellis and Waller (1974). Morphological characteristics of *B. cinerea* isolates were tested by putting mycelial agar plugs (6 mm in diameter) from the colony margin of each isolate of 4-day old cultures on the center of a sterile Czapek's Dox medium plate (9 cm diameter). Three replicates were prepared for each isolate and then incubated for one week at 23°C. Length, width and volume of 200 conidia from each isolate were measured according to Shirane (1989). The conidial volume was determined by measuring conidial dimensions using an objective (40X) of a light microscope, Olympus microscope (BH2), using the following formula:

$$\text{Conidial volume } (\mu m^3) = \frac{L.W^2.\pi}{6}$$

Where L = conidial length (μm), W = conidial width (μm) and π = 3.14159. The conidial shape was examined by a 40X objective of the light microscope and photographed for documentation. Sclerotia were measured for colour, shape, size and number per dish. Mycelial isolate culture (6 mm diameter) of three days was transferred from the colony margin using a sterilized cork-borer to the center of PDA Petri dishes (9 cm); each isolate was measured 21 days after incubation at 23°C.

Pathogenicity test: Detached leaves of lettuce plant (*Lactuca sativa* L. cv. 'Baladi') were prepared to test isolate pathogenicity. Three leaves were prepared as replicates for each isolate, excised from the central part of lettuce head and placed in a plastic box containing moist towels. Mycelial colony plug (6 mm diameter) was removed from the colony margin of each isolate using a sterilized cork-borer and transferred to each lettuce leaf with the mycelial side of culture plug facing the leaf surface. Each plastic box was covered to maintain humidity and then incubated at 23 °C. The measurement of lesion diameter around culture plug was taken daily for 72h. This test was performed in triplicate. The aggressiveness test was conducted according to Abdel Wahab (2015).

Fenhexamid sensitivity assay: Sensitivity of all *B. cinerea* isolates to the hydroxyanilide fungicide, fenhexamid was determined on Czapeek's Dox agar medium amended with a range of fenhexamid concentrations (0.5, 1.5 and 10 mg/L), allowing the growth of resistant isolate but fully inhibiting the growth of sensitive isolates. Fenhexamid (Teldor SC, 500 g/L, Bayer Crop Science) was suspended in sterile distilled water and added to autoclaved media that had cooled to 50°C. The culture plug (6 mm) of four-day old isolate was excised and put on the center of PDA plate amended with different fenhexamid concentrations, previously prepared. Three replicates were prepared for each isolate and then incubated at 23°C for three days. Colony diameter was measured in two perpendicular directions in each plate and the mean was estimated. This test was conducted twice using three replicates for each concentration. The 50% effective concentration (EC50), 50% mycelial growth inhibition, was determined by regressing the relative growth rate (% control) against the log of the fungicide concentration.

Molecular analysis of *Botrytis cinerea* isolates: Single spore culture with the typical morphological characteristic of each *B. cinerea* isolate was transferred to potato dextrose broth (PDB) medium in Erlenmeyer flasks and incubated at 23°C in the dark for 7 days. Genomic DNAs were extracted and purified from harvested mycelia using mini preparation procedure according to Möller *et al.* (1992). *B. cinerea* isolates were identified either by PCR using a pair of specific primers, C729+ and C729- (Rigotti, 2002) (Table 2) or by sequencing the internal transcribed spacer (ITS) regions of fungal ribosomal DNA, using the ITS1/ITS4 primers (White *et al.*, 1990) (Table 2). PCR was carried out in a total volume of 25µl of PCR reaction consisting of 2µl genomic DNA (50 ng/µl), 0.5µl of each primer "Bio-search Technologies" (10µM), 12.5µl Red PCR master mix (Bio-line) and 9.5µl H_2O. The PCR amplification was performed in a thermocycler (Techne-Progene). The reaction was programmed as follows: Initial denaturation at 94°C for 4 min, followed by 35 cycles of denaturation at 94°C for 1 min, annealing at 60°C for 1 min, and extension at 72°C for 1 min, terminating with a final run on 1.5 agarose gel, staining with Red Safe dye and visualized under UV light. A 100-bp DNA marker (Bio-line) was used as a molecular length standard.

Detection of Transposable Elements (TEs) in *Botrytis cinerea* isolates: PCR amplification of the two transposable elements (*Boty* and *Flipper*) using the specific primers BotyF4/BotyR4 and F300/F1550 for each element as demonstrated by Diolez *et al.* (1995) and Levis *et al.* (1997) respectively (Table 2) was conducted as outlined before for Molecular analysis but using the following program: an initial denaturation for 5 min at 95 °C, followed by 40 cycles of denaturation at 94 °C for 1 min, annealing at 60 °C for the primer pair F300/F1550, or 68 °C for the primer pair BotyF4/BotyR4, for 1 min, extension at 72 °C for 1 min (for *boty* primers) or 3 min (for *flipper* primers), and terminated with a final extension at 72 °C for ten min. Amplified products were separated by electrophoresis on 1% agarose gel in TBE, stained with Red Safe dye and visualized under UV light. A molecular length standard of 1 kb DNA ladder (Bio-line) was used.

***Bc-hch* amplification and digestion:** A primer pair 262/520L (Table 2), described by Fournier (Fournier *et al.*, 2003), was used to amplify the *Bc-hch* gene to distinguish between *B. cinerea* and *B. pseudocinerea*. Amplification was performed in a thermocycler (Techne-Progene). The PCR program was as that outlined before for molecular analysis. Restriction fragment length polymorphism (RFLP) was generated through digestion of the 1171 bp product using 2 units of the restriction enzyme *HhaI* (Biolabs, New England), incubated for 90 min at 37°C, resolved on a 2% agarose gel along with a 1Kbp DNA standard ladder marker and visualized under UV light.

Detection of Transposable Elements (TEs) in *Botrytis cinerea* isolates: PCR amplification of the two transposable elements (*Boty* and *Flipper*) using the specific primers BotyF4/BotyR4 and FlipperF300/ Flipper F1550 for each element as demonstrated by Diolez *et al.* (1995) and Levis *et al.* (1997) respectively (Table 2) was conducted as outlined before for Molecular analysis but using the following program: an initial

denaturation for 5 min at 95 ˚C, followed by 40 cycles of denaturation at 94 ˚C for 1 min, annealing at 60 ˚C for the primer pair F300 and F1550, or 68 ˚C for the primer pair BotyF4 and BotyR4, for 1 min, extension at 72 ˚C for 1 min (for *boty* primers) or 3 min (for *flipper* primers), and terminated with a final extension at 72 ˚C for ten min. Amplified products were separated by electrophoresis on 1% agarose gel in TBE, stained with Red Safe dye and visualized under UV light. A molecular length standard of 1 kb DNA ladder (Bio-line) was used.

***Bc-hch* amplification and digestion:** A primer pair Bc-hch262/ Bc-hch520L (Table 2), described by Fournier (Fournier *et al.*, 2003), was used to amplify the *Bc-hch* gene to distinguish between *B. cinerea* and *B. pseudocinerea*. Amplification was performed in a thermocycler (Techne-Progene). The PCR program was as that outlined before for molecular analysis. Restriction fragment length polymorphism (RFLP) was generated through digestion of the 1171 bp product using 2 units of the restriction enzyme *HhaI* (Biolabs, New England), incubated for 90 min at 37°C, resolved on a 2% agarose gel along with a 1Kbp DNA standard ladder marker and visualized under UV light.

Distinction of *B. cinerea* and *B. pseudocinerea*: The Neurospora crassa vegetative incompatibility locus homo-log, Bc-hch, was amplified as described by Fournier *et al.* (2003) using the primers 262 (5-AAGCCCTTCGATGTCTTGGA-3) and 520L (5-ACGGATTCCGAACTAAGTAA-3). Restriction fragment length polymorphisms (RFLPs) were generated through digestion of the 1171 bp product with the restriction enzyme HhaI for 90 min at 37°C, resolved on a 2% agarose gel and visualized by ethidium bromide staining under a UV light.

Phylogenetic analysis of *Botrytis cinerea* isolates using three nuclear genes: Identification of the *B. cinerea* isolates was confirmed by the phylogenetic analysis described by Staats (2004), based on DNA sequencing of the three nuclear genes, glyceraldehyde-3-phosphate dehydrogenase (*G3PDH*), heat-shock protein 60 (*HSP60*) and DNA-dependent RNA polymerase subunit II (*RPB2*) genes using the specific primer pairs G3PDHfor/G3PDHrev, HSP60for/HSP60rev and RPB2for/ RPB2rev, respectively (Table 2) (Staats, 2004). PCR amplification was done on the partial DNA sequences of such three nuclear genes and performed in PCR thermocycler (Techne-Progene). Amplification was carried out in total volume 25µl of PCR reaction as described before under molecular analysis using the following program: Initial denaturation at 94°C for 4 min followed by 35 cycles of denaturation at 94°C for 30 s, annealing at 55°C for 30 s, extension at 72°C for 90 s and a final extension step at 72°C for 10 min for both *HSP60* and *RPB2* gene segments. The same program with an annealing temperature of 64°C was applied to *G3PDH* gene fragment.

Table 2. Sequences of different primer pairs used in the current study.

Primer code	Primer sequence, 5' to 3'	amplicon length (bp)	Reference
C729F	CTGCAATGTTCTGCGTGGAA	700	Rigotti *et al*., 2002
C729R	AGCTCGAGAGAGATCTCTGA		
ITS1	TCCGTAGGTGAACCTGCGG	550	White *et al*., 1990
ITS4	TCCTCCGCTTATTGATATGC		
BotyF4	CAGCTGCAGTATACTGGGGGA	510	Diolez *et al*., 1995
BotyR4	GGTGCTCAAAGTGTTACGGGAG		
F300	GCACAAAACCTACAGAAGA	1250	Levis *et al*., 1997
F1550	ATTCGTTTCTTGGACTGTA		
262	AAGCCCTTCGATGTCTTGGA	1171	Fournier *et al*., 2003
520L	ACGGATTCCGAACTAAGTAA		
G3PDHfor	ATTGACATCGTCGCTGTCAACGA	1000	Staats *et al*., 2005
G3PDHrev	ACCCCACTCGTTGTCGTACCA		
HSP60for	CAACAATTGAGATTTGCCCACAAG	1100	Staats *et al*., 2005
HSP60rev	GATGGATCCAGTGGTACCGAGCAT		
RPB2for	GATGATCGTGATCATTTCGG	1100	Staats *et al*., 2005
RPB2rev	CCCATAGCTTGCTTACCCAT		

The PCR amplicons were separated by agarose gel electrophoresis (1.2 % in TAE 0.5×), purified and sequenced. The phylogenetic analysis was carried out based on a combined dataset of the partial sequences of *RPB2*, *HSP60* and *G3PDH* that were obtained from the tested *B. cinerea* isolates. Molecular and phylogenetic analyses were performed using MEGA6 software, version 6 (Tamura *et al.*, 2013). The missing data and nucleotide gaps in the DNA sequences were deleted. The phylogeny tree was constructed using the Neighbour joining method and individually tested with a bootstrap of 1000 replicates to achieve the reliability of any given branch pattern in each Neighbour joining tree.

Statistical analysis: All data that scored from morphological features, mycelial growth rates, pathogenicity and fenhexamid sensitivity assays were tested by analysis of variance (ANOVA) to determine the significant differences. Data means were treated using the least significant difference test at $P = .05$ level.

RESULTS

Pathogen isolation from grape and strawberry naturally infected with grey mold: Diseased plant parts were cultured on the selective medium, m1KERS for isolation of the causal agent, microscopically identified as *B. cinerea*. Data presented in Table 1 showed that *B. cinerea* was identified in 51 isolates which included 25 and 26 isolates collected from grape and strawberry, respectively.

Phenotypic diversity of *Botrytis cinerea* isolates: Variation among all isolates of *B. cinerea* was achieved by morphological and microscopical characterization. The results obtained showed that *B. cinerea* isolates varied in growth texture (Table 3) and were categorized as compact, heavy warty, light warty, fluffy and watery. Conidial dimensions differed significantly among isolates, ranging from 10.6 to 12.7 µm in length, 7.3 to 8.9 µm in width and 297.6 to 491.1µm^3 in volume (Table 3). Conidia of all isolates were described as oval shape and sclerotia characteristics like size, number and distribution pattern were determined for each plate. Data obtained indicated that sclerotia varied in shape with two types, being cerebriform in all isolates except BCS102, BCS105 and BCS110 whose sclerotia were flat (Table 3).

Table 3. Phenotypic characteristics of *Botrytis cinerea* isolates collected from grape and strawberry.

						Dimensions of Conidia (µM)**			
Isolate	Growth Texture	Sclerotial Shape	Sclerotia Distribution	No. of Sclerotia/ Plate*	Conidial Shape	Length	Width	L/W ratio	Conidial Volume (µM^3)
BCG101	Compact	Cerebriform	Large - irregularly	81.0±2.0	Ovate	11.2±0.9	8.4±0.8	1.4±0.2	413.1±68.5
BCG102	Compact	Cerebriform	Large - irregularly	76.3±3.1	Ovate	11.9±0.3	8.6±1.1	1.4±0.2	466.7±13.3
BCG103	Compact	Cerebriform	Large - irregularly	70.7±1.5	Ovate	10.8±0.6	8.2±0.7	1.3±0.2	377.7±66.9
BCG104	Compact	Cerebriform	Large - irregularly	70.0±1.0	Ovate	12.1±0.7	8.7±0.8	1.4±0.2	475.4±84.6
BCG105	Compact	Cerebriform	Large - irregularly	75.0±4.6	Ovate	10.7±0.5	7.3±0.6	1.5±0.2	297.6±44.9
BCG106	Light warty	Cerebriform	small - scattered	162.7±2.5	Ovate	11.7±0.6	8.9±0.7	1.4±0.1	444.0±86.0
BCG107	Light warty	Cerebriform	small - scattered	169.7±3.5	Ovate	12.5±0.7	8.3±0.6	1.5±0.1	457.7±70.9
BCG108	Light warty	Cerebriform	small - scattered	182.0±2.7	Ovate	11.4±0.6	8.2±0.7	1.4±0.2	402.1±78.1
BCG109	Light warty	Cerebriform	small - scattered	155.3±4.5	Ovate	11.7±0.7	8.4±0.6	1.4±0.1	433.6±69.6
BCG110	Light warty	Cerebriform	small - scattered	177.7±5.1	Ovate	11.4±0.5	8.2±0.7	1.4±0.1	405.6±64.8
BCG111	Light warty	Cerebriform	small - scattered	155.3±2.5	Ovate	11.8±0.6	8.4±0.7	1.4±0.4	434.9±66.8
BCG112	Light warty	Cerebriform	small - scattered	186.7±3.5	Ovate	10.7±0.7	8.1±0.5	1.3±0.1	363.3±39.6
BCG113	Light warty	Cerebriform	small - scattered	191.3±1.5	Ovate	12.1±0.6	8.5±0.5	1.4±0.1	458.7±62.7
BCG114	Light warty	Cerebriform	small - scattered	162.7±2.1	Ovate	10.6±0.6	8.2±0.6	1.3±0.1	375.9±62.7

BCG115	Light warty	Cerebriform	small - scattered	192.0±2.0	Ovate	11.8±0.6	8.9±0.9	1.3±0.2	491.1±106.7
BCG116	Fluffy	Cerebriform	small - scattered	185.0±2.7	Ovate	11.5±0.6	8.3±0.7	1.4±0.1	416.1±69.5
BCG117	Fluffy	Cerebriform	small - scattered	173.0 ±2.0	Ovate	11.4±0.5	7.9±0.5	1.4±0.1	377.6±59.9
BCG118	Fluffy	Cerebriform	small - scattered	183.7±3.1	Ovate	10.7±0.5	7.7±0.6	1.4±0.1	335.8±52.6
BCG119	Fluffy	Cerebriform	small - scattered	159.3 ±2.1	Ovate	11.9±0.5	8.1±0.7	1.5±0.1	413.6±75.5
BCG120	Fluffy	Cerebriform	small - scattered	168.7±4.2	Ovate	11.5±0.7	8.1±0.6	1.4±0.2	397.9±55.1
BCG121	Fluffy	Cerebriform	small - scattered	191.7±1.5	Ovate	11.4±0.5	8.3±0.6	1.4±0.1	410.8±36.4
BCG122	Fluffy	Cerebriform	small - scattered	174.7±4.1	Ovate	10.8±0.5	7.9±0.3	1.3±0.1	352.0±39.2
BCG123	Fluffy	Cerebriform	small - scattered	154.0±5.6	Ovate	11.9±0.5	8.3±0.6	1.5±0.1	431.4±64.5
BCG124	Fluffy	Cerebriform	small - scattered	178.7±4.2	Ovate	12.7±0.6	8.2±0.3	1.6±0.1	445.3±67.0
BCG125	Fluffy	Cerebriform	small - scattered	174.3±4.2	Ovate	11.5±0.5	8.3±0.6	1.4±0.1	413.6±63.5
BCS101	Heavy warty	Cerebriform	Large - irregularly	201.3±2.5	Ovate	11.5±0.5	8.3±0.6	1.4±0.1	419.6±66.2
BCS102	Watery	Flat	Large in circle	187.0±3.5	Ovate	11.7±0.6	7.9±1.0	1.5±0.2	386.6±98.2
BCS103	Watery	Cerebriform	Large - irregularly	193.3±4.2	Ovate	11.2 ±0.9	8.1±0.7	1.4±0.2	387.1±67.8
BCS104	Watery	Cerebriform	Large - irregularly	164.3±5.1	Ovate	12.2±0.9	8.6±0.8	1.4±0.2	467.8±90.4
BCS105	Watery	Flat	Large in circle	178.3±4.0	Ovate	10.7±0.7	8.2±1.0	1.3±0.2	379.7±101.1
BCS106	Watery	Cerebriform	Large in circle	194.7±3.8	Ovate	11.9±0.8	8.3±0.8	1.5±0.2	428.8 ±70.9
BCS107	Watery	Cerebriform	Large - irregularly	184.3±3.2	Ovate	11.8±0.8	8.3±1.2	1.4±0.2	435.2 ±127.9
BCS108	Heavy warty	Cerebriform	Large - irregularly	195.7±3.1	Ovate	11.2±0.7	8.1±1.0	1.4±0.2	390.8 ±109.3
BCS109	Heavy warty	Cerebriform	Large - irregularly	181.0±2.0	Ovate	12.2±0.7	8.4±0.9	1.5±0.1	465.9 ±135.1
BCS110	Watery	Flat	Large in circle	176.0±3.6	Ovate	11.4±0.6	8.2±0.7	1.4±0.1	408.2±77.6
BCS111	Watery	Cerebriform	Large - irregularly	90.0±1.0	Ovate	11.5±0.6	7.9±0.4	1.5±0.1	382.6±54.5
BCS112	Watery	Cerebriform	Large - irregularly	82.7±4.0	Ovate	10.8±0.7	7.4±0.7	1.5±0.1	312.9±78.9
BCS113	Watery	Cerebriform	Large - irregularly	85.3±6.4	Ovate	11.9±0.8	8.2±0.7	1.5±0.1	421.7±92.6
BCS114	Fluffy	Cerebriform	Large - irregularly	93.3±3.2	Ovate	11.3±0.8	7.9±0.9	1.4±0.2	383.8±99.1
BCS115	Fluffy	Cerebriform	Large - irregularly	97.3±4.7	Ovate	11.8±0.8	8.2±0.7	1.5±0.1	422.7±86.8
BCS116	Fluffy	Cerebriform	Large - irregularly	75.3±4.5	Ovate	12.1±0.8	8.2±0.9	1.5±0.2	430.6±100.3
BCS117	Watery	Cerebriform	Aggregate - center	-	Ovate	11.2±0.6	7.9±0.8	1.4±0.2	378.6 ±77.7
BCS118	Fluffy	Cerebriform	Large - irregularly	90.3±1.5	Ovate	11.8±0.7	8.6±1.0	1.4±0.1	462.1±127.1
BCS119	Fluffy	Cerebriform	Large in circle	72.7±5.0	Ovate	10.9±0.9	8.1±0.7	1.4±0.1	377.9 ±77.0
BCS120	Fluffy	Cerebriform	Large in circle	63.0±3.6	Ovate	11.1±0.8	7.6±0.9	1.5±0.1	339.6±108.9
BCS121	Fluffy	Cerebriform	Large in circle	65.7±4.0	Ovate	11.7±0.7	8.3±1.1	1.4±0.2	428.4 ±117.3
BCS122	Fluffy	Cerebriform	Large - irregularly	17.7±1.5	Ovate	11.5±0.6	8.2±1.1	1.4±0.2	410.9±115.9
BCS123	Fluffy	Cerebriform	Large - irregularly	21.7±2.5	Ovate	11.2±0.8	7.8±1.1	1.5±0.2	365.4±117.1
BCS124	Fluffy	Cerebriform	Large - irregularly	27.0±2.7	Ovate	11.8± 0.7	8.2±1.2	1.5±0.2	428.7±131.6
BCS125	Fluffy	Cerebriform	Large - irregularly	28.3±1.5	Ovate	11.8± 0.7	8.4±0.8	1.4±0.1	438.4 ±89.2
BCS126	Fluffy	Cerebriform	Large - Irregularly	24.0±2.7	Ovate	11.2± 0.6	8.2±0.8	1.4±0.1	402.5±91.2

*, All data are means of triplicate measurements ± standard deviation (SD) at $LSD_{.05}$, ** All data are means of 20 conidial measurements ± standard deviation (SD) at $LSD_{.05}$.

Four categories of the sclerotial pattern were recognized and these were: large irregular, large in circle, small/scattered and aggregate in the center of culture plate. A different number of sclerotia was observed per culture plate and ranged from 17.7 to 201.3 sclerotia/plate. In addition, the mycelial growth rate ranged from 0.3 to 4.9cm (Table 4).

Pathological and molecular pattern of *Botrytis cinerea* isolates: The degree of virulence of 51 isolates of *B. cinerea* collected from grape and strawberry was assessed by using detached lettuce leaves (see materials and methods). A significant difference among isolates depending on their aggressiveness in terms of lesion diameter was observed (Table 4). Statistical analysis showed that isolates differed significantly in lesion size with diameter ranging from 0.3 to 5.1 cm. Isolates were divided, depending on their virulence, into three categories: highly virulent with a lesion diameter ranging from >2.5 cm to 5.1 cm (43.1%); moderately virulent with a lesion ranging from >1 to 2.5 cm (43.1%); low virulent with a lesion diameter ranging from 0.3 to 1 cm (13.7%). Results of typing twenty-five isolates of *B. cinerea* from grape and twenty-six isolates from strawberry for TEs presence using either the specific primers BotyF4 & BotyR4 to amplify *boty* element or F300/F1550 to amplify *flipper* element showed four TEs types (Table 4).

Table 4. Pathological and TE patterns of *Botrytis cinerea* isolates from grape and strawberry.

Isolate	MGR (cm/d)*	Lesion diameter (cm)**	Type***	Isolate	MGR (cm/d)*	Lesion diameter (cm)**	Type***
BCG101	2.1±0.2hi	2.4±0.1j	T	BCS102	2.3 ± 0.1efg	1.9±0.1efghi	T
BCG102	2.6±0.2gf	2.5±0.1ij	B	BCS103	0.3±0.1l	1.0±0.2jk	F
BCG103	3.1±0.1cde	2.9±0.2fgh	T	BCS104	1.6±0.2jk	2.2±0.8abcdef	B
BCG104	2.9±0.4def	0.3±0.1k	V	BCS105	1.9±0.1hgi	1.6±1.3fghijk	B
BCG105	3.4±0.4c	5.1±0.2a	B	BCS106	2.3±0.1efg	1.4±0.2hijk	T
BCG106	1.5±0.0kl	3.1±0.6fg	B	BCS107	2.1±0.6fghi	2.2±0.8abcdef	F
BCG107	3.0±0.1def	3.9±0.4bcd	T	BCS108	1.9±0.1hij	2.0±0.4cdefghi	T
BCG108	3.1±0.3cde	2.7±0.3hij	T	BCS109	0.4±0.1l	1.8±0.1efghij	T
BCG109	2.7±0.1fg	3.7±0.4cde	B	BCS110	2.5 ± 0.1de	2.7±0.3abcd	B
BCG110	4.0±0.3b	0.3±0.0k	V	BCS111	3.3 ± 0.3b	2.8±0.2ab	F
BCG111	1.6±0.2kl	2.9±0.2gh	B	BCS112	2.4 ± 0.0def	1.6±0.1fghijk	F
BCG112	4.7±0.2a	4.1±0.3b	T	BCS113	3.1 ± 0.4b	1.4±0.0hijk	T
BCG113	1.9±0.5ij	2.9±0.0gh	T	BCS114	1.9 ± 0.3hij	1.8±0.1efghi	T
BCG114	1.0±0.4m	2.8±0.2hi	T	BCS115	0.4 ± 0.2l	2.4±0.2abcdef	T
BCG115	4.5±0.0a	3.3±0.3ef	T	BCS116	1.8 ± 0.2ijk	2.7±0.8abc	B
BCG116	4.9±0.1a	4.9±0.3a	F	BCS117	4.1 ± 0.2a	2.1±0.1bcdefgh	B
BCG117	3.4±0.2c	2.9±0.1fgh	T	BCS118	2.2 ± 0.1efgh	1.6±0.3ghijk	V
BCG118	1.2±0.1lm	0.4±0.2k	F	BCS119	2.4 ± 0.1def	0.9±0.1k	B
BCG119	2.2±0.1hi	2.6±0.1hij	B	BCS120	3.1 ± 0.2de	1.6±0.1ghijk	B
BCG120	3.2±0.2cd	4.0±0.3bc	B	BCS121	3.0 ± 0.2b	1.3±0.2ijk	B
BCG121	3.3±0.1b	3.9±0.2bcd	T	BCS122	3.0 ± 0.2bc	0.9±0.1k	T
BCG122	3.9±0.2kj	5.1±0.3a	T	BCS123	0.3 ± 0.0l	2.1±0.1abcdefgh	T
BCG123	1.7±0.1gh	0.4±0.1k	B	BCS124	2.5 ± 0.1def	1.9±0.5cdefghi	B
BCG124	2.5±0.2gh	3.6±0.2de	T	BCS125	0.3±0.1 l	2.4±0.5abcde	B
BCG125	2.7±0.2gef	3.9±0.1bcd	F	BCS126	1.5±0.1k	2.4±0.8abcde	F
BCS101	2.7 ± 0.4cd	2.1±0.2bcdefg	T				

*, MGR: mycelial growth rate. All data for growth rate of isolates collected from strawberry and grape are means of triplicate measurements ± standard deviation (SD) at $LSD_{.05}$, respectively. **, data for lesion diameter are means of triplicate measurements ± standard deviation (SD) at $LSD_{.05}$ after 72h of infection. ***, transposable element type, B, only *boty*, F, only *flipper*, T, *transposa*, V, *vacuma*. $^{a\text{-}m}$, means in a column followed by a different letter differ significantly (p=.05). Data were means ± SD of triplicate measurements.

For *boty* detection, PCR generated 510 bp, whereas, PCR revealed the expected 1250 bp for flipper element. Among 51 isolates tested, 22 have the two transposable elements, *boty* and *flipper* (*transposa* type), which indicated that *transposa* isolates were predominant (43.1%) in almost all of *B. cinerea* populations isolated from grape and strawberry. While, 18 have only *boty* element (*boty* type, 35.3%), 8 have only *flipper* element (*flipper* type, 15.7%) and 3 have neither of these two elements (*vacuma* type, 5.9%).

Sensitivity of *Botrytis cinerea* isolates to fenhexamid: The results revealed that all *B. cinerea* isolates were highly sensitive to fenhexamid. EC50 of strawberry isolates was less than 0.1µg fenhexamid ml^{-1} (Figure 1). EC50 values ranged from 0.012- 0.078 and 0.014 - 0.084µg fenhexamid /ml for *B. cinerea* isolates collected from both strawberry and grape, respectively (Figures 2 and 3).

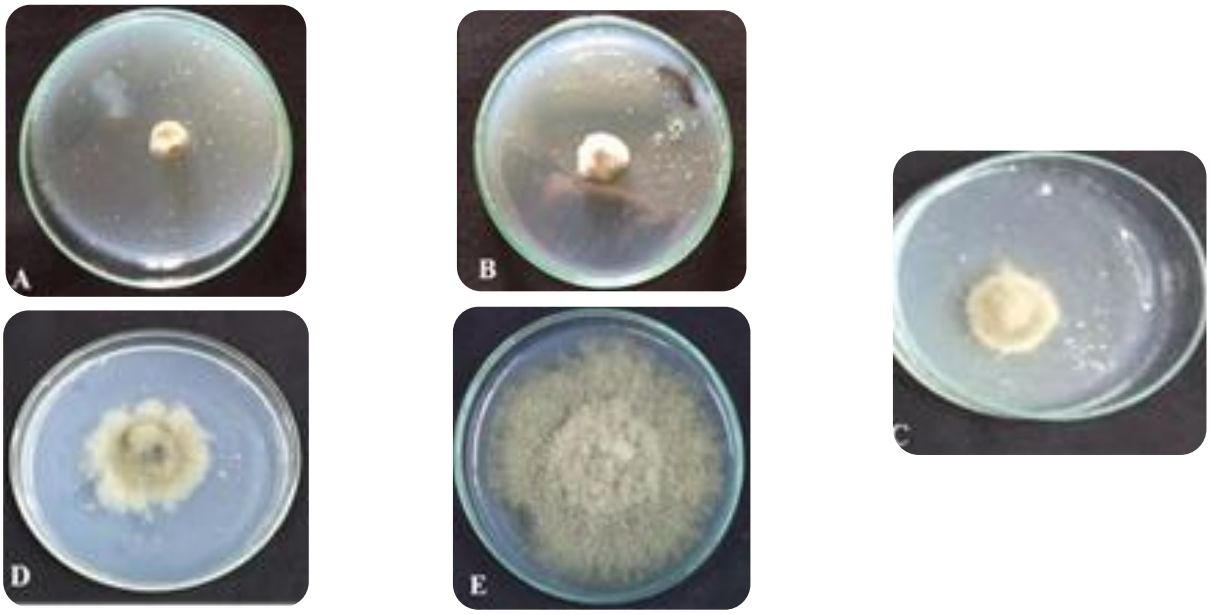

Figure 1. Effect of different fenhexamid concentrations on the mycelial growth of *Botrytis cinerea* isolate BCS13. One µg/ml (A), 0.1µg/ml (B), 0.05µg/ml (C), 0.025µg/ml (D) and 0.00 µg/ml, control (E).

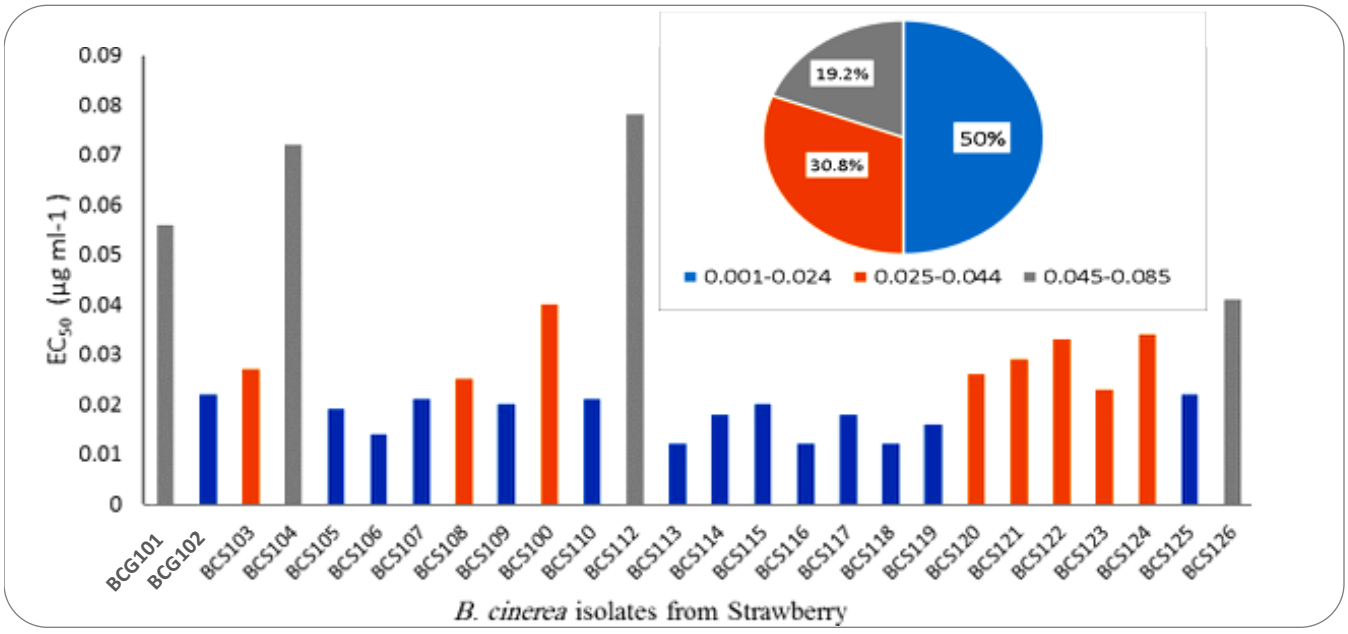

Figure 2. Sensitivity of *Botrytis cinerea* isolates from strawberry to fenhexamid, expressed as EC50 (µg ml^{-1}). The inset is a pie chart showing the percentage of different categories of isolate sensitivity to fenhexamid.

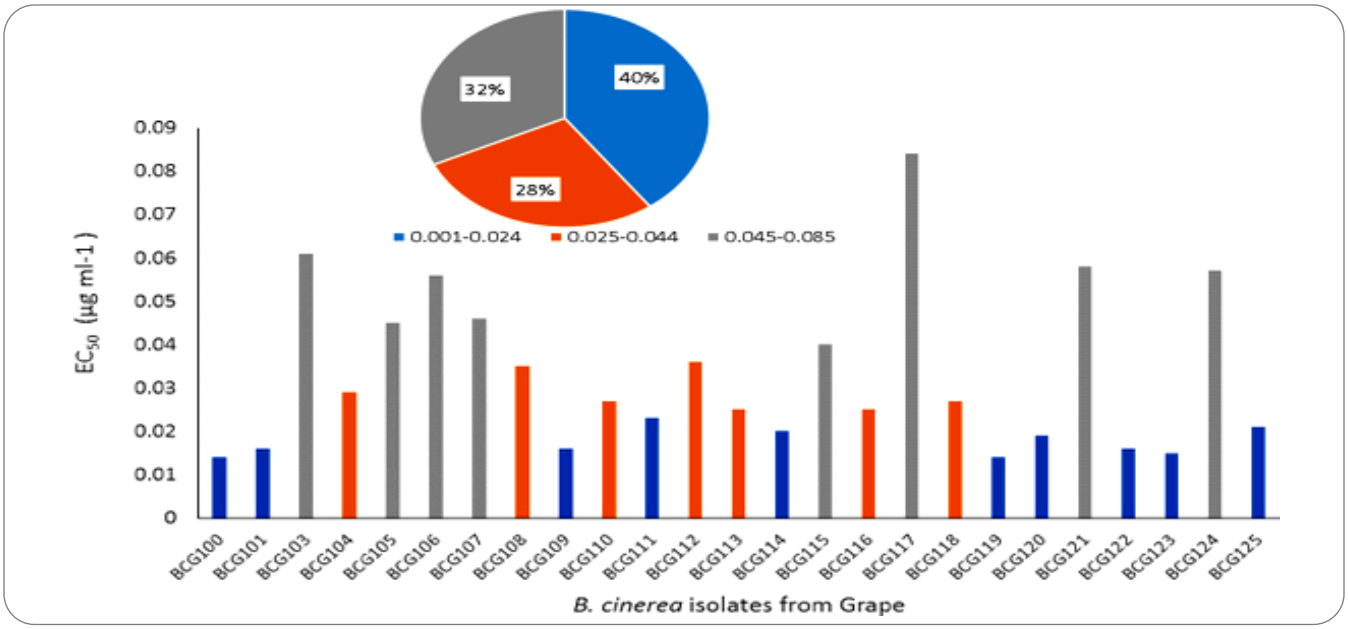

Figure 3. Sensitivity of *Botrytis cinerea* isolates from grape to fenhexamid, expressed as EC50 (µg ml-1). The inset is a pie chart showing the percentage of different categories of isolate sensitivity to fenhexamid.

The highest sensitive isolates were BCS113, BCS116 and BCS118 from strawberry where EC50 value was as low as 0.012µg/ml, BCG101 and BCG119 from grape where EC50 value was 0.014µg/ml. The lowest sensitive isolate from strawberry was BCS112 where EC50 value was 0.078µg/ml and BCG117 from grape where EC50 value was 0.084 µg/ml.

Molecular divergence of *Botrytis* isolates using the three nuclear genes: Molecular identification of all isolates by PCR using a pair of specific primers, C729+ and C729- (Rigotti *et al.,* 2002) revealed a single band of 700 bp (data not shown) and this confirmed that all isolates were *B. cinerea*. The PCR amplification targeting the three nuclear genes of the two isolates, BCS101 and BCG101, using specific primers (Table 2) revealed amplicons of approximately 1000, 1100 and 1100 bp, respectively (Figure 4), corresponding to a partial sequence of the three housekeeping genes: heat-shock protein 60 (*HSP60*), glyceraldehyde-3- phosphate dehydrogenase (*G3PDH*) and DNA-dependent RNA polymerase subunit II (*RPB2*).

DNA sequencing and phylogenetic analysis of the three nuclear genes: Sequence analysis of the amplified products revealed that the two isolates tested, BCS101 and BCG101, were *B. cinerea* based on the percentage of identity which ranged from 98 to 100% using BLAST search (GenBank accession no. MH752681, MH752682, MH752683, MH752684 and MH752685).

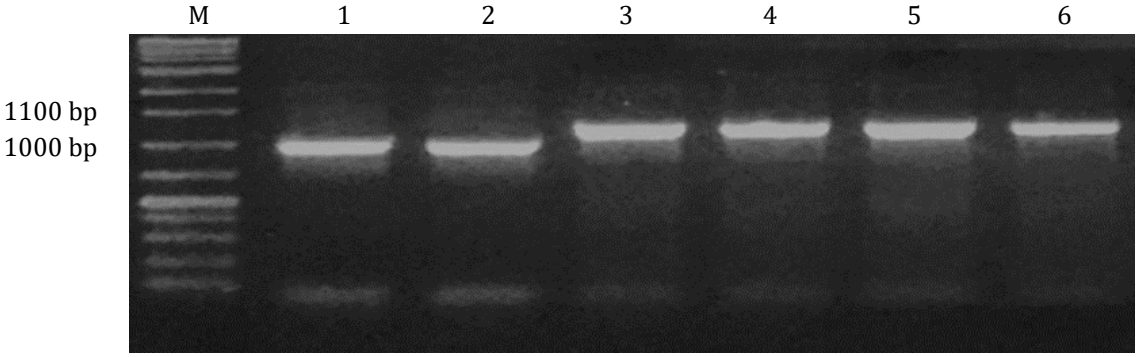

Figure 4. PCR amplification of the three nuclear genes (*G3PDH*, *HSP60* and *RPB2*) produced an amplicon of approximately 1000, 1100 and 1100 bp in two isolates (BCS101 and BCG101) of *B. cinerea* using specific primers. Left lane (M), is a 1Kbp DNA ladder marker. Lanes 1 to 6 are loaded with samples representing such two isolates.

The phylogenetic analysis of the current isolates clustered with *B. cinerea* (Figures 5, 6 and 7) and showed that the Egyptian isolates were clearly distinguished from other *Botrytis* spp. deposited in the GenBank, including *B. pseudocinerea*, *B. fabae*, *B. sinoviticola, B. fabiopsis*, *B. squamosa*, *B. sinoallii*, *B. pelargonii,* and *B. tulipae*.

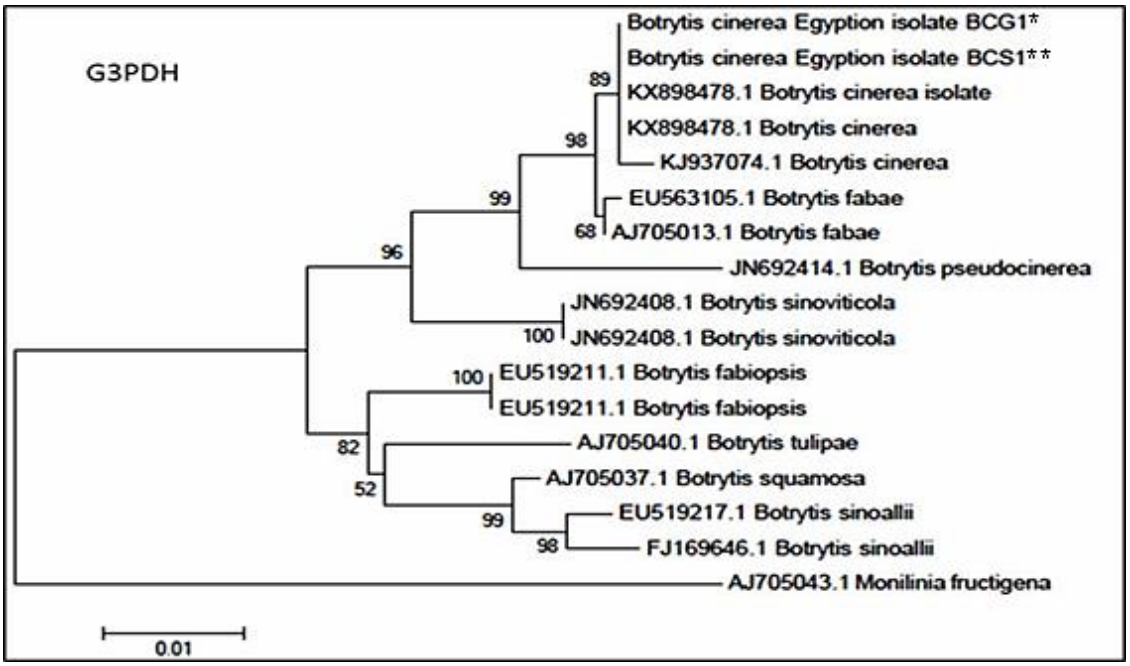

Figure 5. Molecular phylogenetic tree obtained through the Neighbor-joining tree method using MEGA6 software program based on *G3PDH* gene of isolates under study and other *Botrytis* spp. isolates deposited in the GenBank. * and **: Isolates BCG1 and BCS1 corresponding to isolates BCG101 and BCS101, respectively. Bootstrap support values (%) resulted from 1000 replicates are shown at each branch point. *Monilinia fructigena* served as an outgroup fungus.

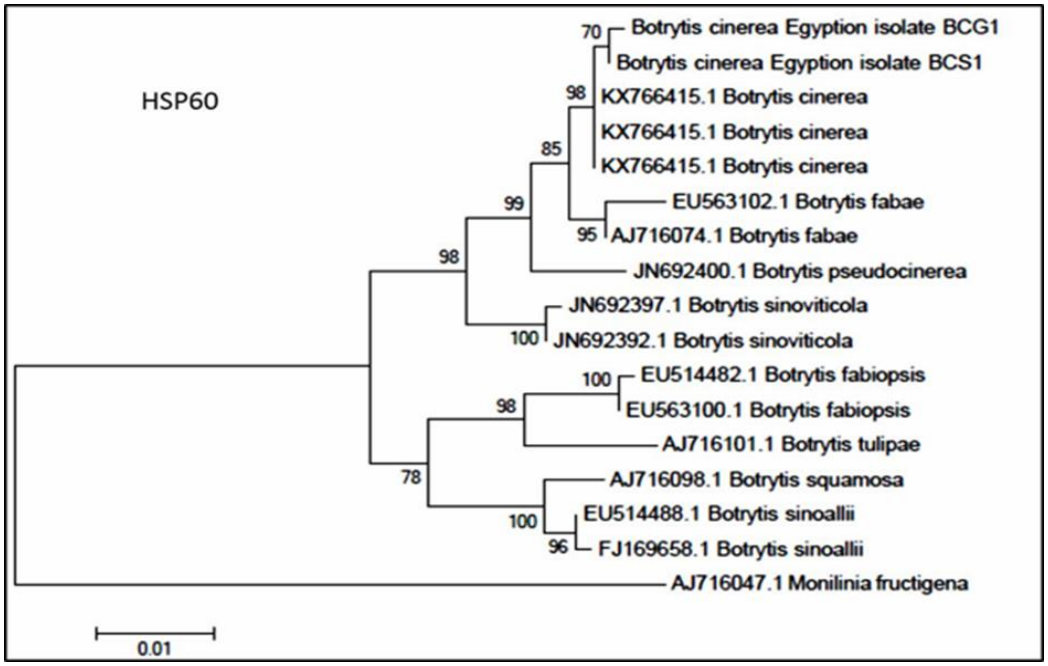

Figure 6. Molecular phylogenetic tree obtained through the Neighbor-joining tree method using MEGA6 software program based on *HSP60* gene of isolates under study and other *Botrytis* spp. isolates retrieved from GenBank. Bootstrap support values (%) resulted from 1000 replicates are shown at each branch point. *Monilinia fructigena* served as an outgroup fungus.

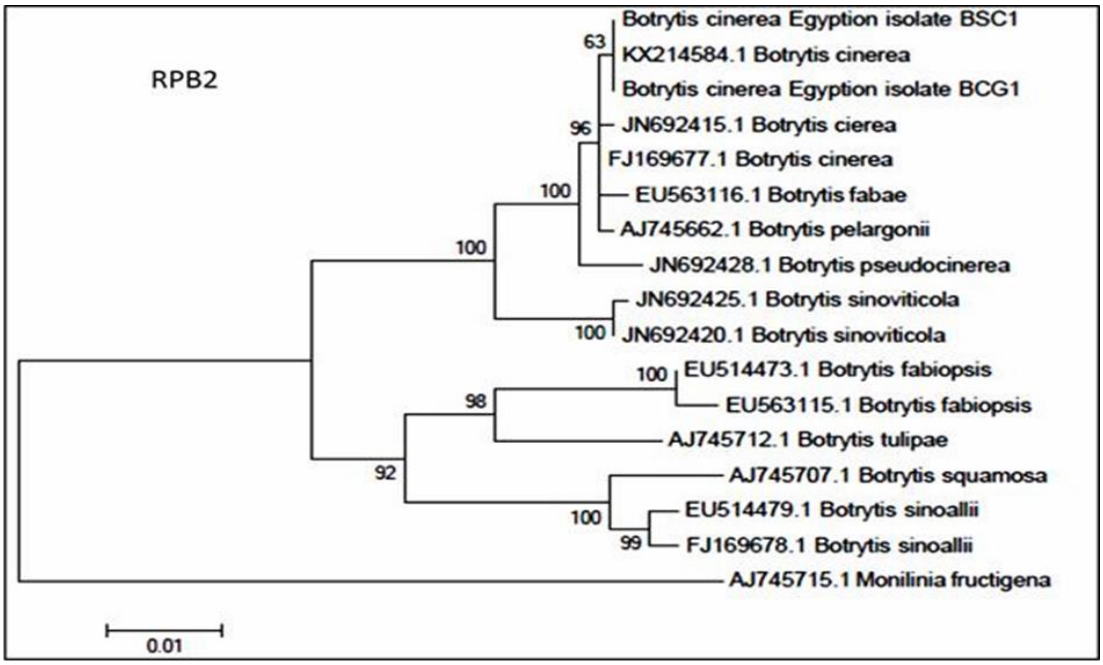

Figure 7. Molecular phylogenetic tree obtained through the Neighbor-joining tree method using MEGA6 software program based on *RPB2* gene of isolates under study and other *Botrytis* spp. isolates retrieved from GenBank. Bootstrap support values (%) resulted from 1000 replicates are shown at each branch point. *Monilinia fructigena* served as an outgroup fungus.

***Bc-hch* amplification and digestion:** In order to distinguish between *B. cinerea* and *B. pseudocinerea*, the current isolates were tested by PCR using Bc-hch specific primers followed by digestion of the *Bc-hch* locus with *HhaI* enzyme. PCR analysis with Bc-hch specific primers (262/520L), revealed a fragment of 1171 bp corresponding to the region of the *Bc-hch* gene, in five grape isolates (BCG103, BCG106, BCG117, BCG121, BCG124) and three strawberry isolates (BCS101, BCS104, BCS112) (Figure 8A). The isolates under study demonstrated that they were *B. cinerea* as they revealed a 517 bp amplicon after using the restriction enzyme, *HhaI*. The PCR amplicons resulted from the amplification of the *Bc-hch* gene were digested with the restriction enzyme *HhaI* indicated that they belonged to Group II (Figure 8B).

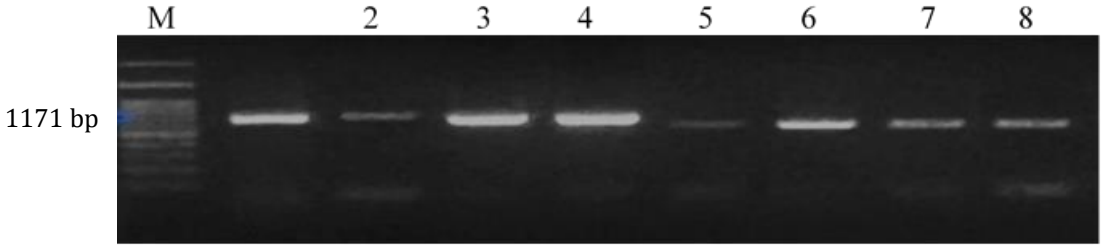

Figure 8. A, PCR amplicons of 1171 bp using Bc-hch specific primers (262/520L).

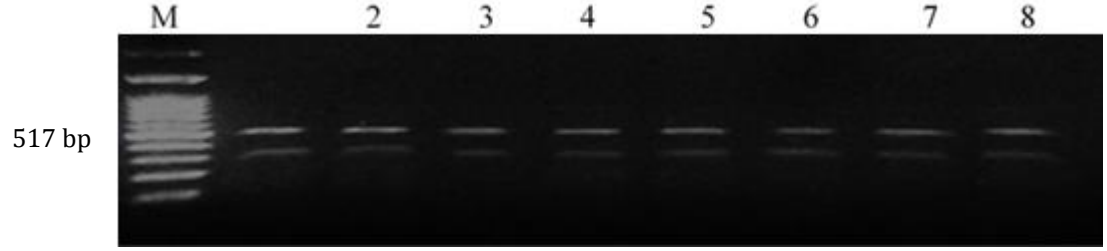

Figure 8. B, Restriction digestion of PCR amplicons with the restriction enzyme *HhaI*.

Left lanes (M), 1Kbp ladder marker, lanes 1 to 5 loaded with samples corresponding to five grape isolates (BCG103, BCG106, BCG117, BCG121, BCG124, respectively) and lanes 6 to 8 corresponding to three strawberry isolates (BCS101, BCS104 and BCS112, respectively).

DISCUSSION

Variability of *B. cinerea* isolates was evident among isolates collected from two different host plants, grape and strawberry which were grown in various geographic locations in Egypt. When the variation in virulence was tested, isolates were found to lie in three categories: high, moderate and low virulence. However, no correlation was found between virulence and geographic origin. In contrast, a great variation in aggressiveness was observed among *B. cinerea* isolates collected from the same location. This could be due to various reasons including the ability of *B. cinerea* conidia to disseminate over long distances and the phenomenon of gene flow that may circumvent geographical differentiation (Mirzaei *et al.*, 2009). However, no specific pattern was observed between isolate location and morphological features. Results of transposable elements (TEs) typing of *B. cinerea* isolates from grape and strawberry indicated that *transposa* type was predominant (43.1%) in almost all of *B. cinerea* populations studied, a finding that was previously reported by Esterio *et al.* (2011) followed by *boty* (35.3%), *flipper* (15.7%) and *vacuma* (5.9%) types. This distribution frequency of the four transposon types was in agreement with that reported in a recent study (Abdel Wahab, 2015), but differed from those published elsewhere (Samuel *et al.*, 2012; Kumari *et al.*, 2014). This discrepancy may be due to a number of reasons such as differences in population size, location, time of sampling, plant species, plant growth stage and saprotrophic versus pathogenic fitness. In fact, TEs typing had been used as a qualitative marker to study genetic variation (Giraud *et al.*, 1999; Daboussi and Capy, 2003; Abdel Wahab, 2015), and this led them to become a molecular character of all isolates of *B. cinerea* from strawberry and grape. The four TE types were recognized on the basis of TE distribution in *B. cinerea* isolates and had previously been documented (Muñoz *et al.*, 2010; Wahab *et al.*, 2019). The current study demonstrated a correlation between the distribution of TEs and some fungal characters such as the location, host plant and virulence. All BCG isolates having *flipper* type were collected from grape growing in Alexandria, while the majority of BCS isolates which were collected from EL-Behiera have revealed all TE types. Whereas the mean conidial dimensions were the same in *transposa*, *boty*, *flipper* and *vacuma* isolates, virulence testing revealed that all BCG isolates with *transposa* type were highly virulent except BCG101 isolate which demonstrated moderate virulence. Similarly, while all BCS isolates with *transposa* type were moderately virulent, BCS122 isolate exhibited weak virulence. As to *vacuma* type, BCG isolates were shown to be weak in virulence, but BCS isolates were found to be moderate in this respect. These results suggested that *transposa* isolates had higher virulence potential as compared to *vacuma* ones. These findings are in agreement with those previously reported (Martinez *et al.*, 2005; Schilling *et al.*, 2013; Samuel *et al.*, 2012; Kumari *et al.*, 2014; Abdel Wahab, 2015; Pande *et al.*, 2010). Noticeably, there was no diversity in virulence among isolates on the basis of location. However, variation among isolates collected from different geographical locations were characterized based on their sensitivity towards fenhexamid. Results revealed that all isolates, obtained from both strawberry and grape, were fenhexamid-sensitive with EC50 values ranging between 0.012 - 0.084 µg/ml, indicating fenhexamid sensitivity (Rodríguez *et al.*, 1997), and may suggest that all isolates were related to *B. cinerea* group II (Albertini *et al.*, 2002; Albertini and Leroux, 2004; Leroux *et al.*, 2002; Leroux *et al.*, 2010). However, no correlation was found between sensitivity to fenhexamid and the possession of TE, and this is consistent with previous studies (Giraud *et al.*, 1999; Albertini *et al.*, 2002), but contradictory with others (Fournier *et al.*, 2002; Leroux *et al.*, 2002). The inability to isolate a fenhexamid-resistant isolate may suggest that fenhexamid-resistance is absent among *Botrytis cinerea* populations in Egypt. However, this preliminary observation remains to be confirmed by involving more isolates from more host plants and more geographical locations. This evidence is supported by the fact that fenhexamid is still effective in controlling *B. cinerea* infections in Egypt. It might be relevant to indicate that RFLP and sequence analyses of all isolates investigated in this study demonstrated no polymorphism among *Botrytis cinerea* isolated from Egypt. Additionally, the genetic distance reported here between the Egyptian isolates and the GenBank accessions and the fact that they constituted a separate divergent group when phylogenetic analysis was conducted may help to explain the widespread sensitivity to fenhexamid commonly encountered among Egyptian isolates of *B. cinerea*. Although the results reported here were derived from a large number of samples isolated from various host plants growing in different geographical locations, no divergence events were observed among isolates. Combining the results of fenhexamid sensitive isolates with molecular analysis of

population structure could help in planning a suitable control measures in which effective disease management would be achieved by applying fungicides in rotation with less chances of developing resistant variants. However, future studies involving more isolates from new other locations and plant species may still be needed to establish a clearer picture of variation among *B. cinerea* isolates in Egypt.

ACKNOWLEDGEMENTS

The authors would like to thank Dr. Mahmoud Magdy, Department of Genetics, Ain Shams University, for his valuable assistance in phylogenetic analysis. This research was partially supported by the Science and Technology Development Fund (STDF), Egypt, Grant No. 2131. The modified selective medium was registered as a patent (no. 2012091520) from Academ y of Scientific Research and Technology (ASRT), Ministry of Scientific Research, Cairo, Egypt.

REFERENCES

Abdel Wahab, H. 2015. Characterization of Egyptian Botrytis cinerea Isolates from Different Host Plants. Advances in Microbiology, 05: 177-89. https://doi.org/10.4236/aim.2015.53017

Abdel Wahab, H. and N. Helal. 2013. Evaluation of Pre-Harvest Bioagent Applications for both Production and Biological Control of Onion and Strawberry Plants under Natural Botrytis Infections. African Journal of Plant Science and Biotechnology, 7: 64-69.

Ahmed, M. F. and E. I. Naim. 1993. Effect of irrigation interval on consumptive use, water use efficiency and crop coefficient of sunflower. Journal of Agricultural Sciences, 1: 1-15.

Albertini, C. and P. Leroux. 2004. A *Botrytis cinerea* Putative 3-keto Reductase Gene (ERG27) that is Homologous to the Mammalian 17 - Hydroxysteroid Dehydrogenase type 7 gene (17 - HSD7). European Journal of Plant Pathology, 110: 723-33. https://doi.org/10.1023/b:ejpp.0000041567.94140.05

Albertini, C., G. Thebaud, E. Fournier and P. Leroux. 2002. Eburicol 14α-demethylase gene (CYP51) polymorphism and speciation in *Botrytis cinerea*. Mycological Research, 106: 1171-78. https://doi.org/10.1017/s0953756202006561

Buttner, P., F. Koch, K. Voigt, T. Quidde, S. Risch, R. Blaich, B. Brckner and P. Tudzynski. 1994. Variations in ploidy among isolates of *Botrytis cinerea*: implications for genetic and molecular analyses. Current Genetics, 25: 445-50. https://doi.org/10.1007/bf00351784

Chardonnet, C. O., C. E. Sams, R. N. Trigiano and W. S. Conway. 2000. Variability of three isolates of *Botrytis cinerea* affects the inhibitory effects of calcium on this fungus. Phytopathology, 90: 769-74.

Daboussi, M.-J. and P. Capy. 2003. Transposable Elements in Filamentous Fungi. Annual Review of Microbiology, 57: 275-99. https://doi.org/10.1146/annurev.micro.57.030502.091029

Diolez, A., F. Marches, D. Fortini and Y. Brygoo. 1995. Boty, a long-terminal-repeat retroelement in the phytopathogenic fungus *Botrytis cinerea*. Applied and Environmental Microbiology, 61: 103-08.

Dufresne, M., A. Hua-Van, H. Abd el Wahab, S. B. M'Barek, C. Vasnier, L. Teysset, G. H. J. Kema and M.-J. Daboussi. 2006. Transposition of a Fungal Miniature Inverted-Repeat Transposable Element Through the Action of a Tc1-Like Transposase. Genetics, 175: 441-52. https://doi.org/10.1534/genetics.106.064360

Ellis, M. and J. Waller. 1974. Sclerotinia fuckeliana (conidial state: *Botrytis cinerea*). CMI descriptions of pathogenic fungi and bacteria.

Esterio, M., G. Muñoz, C. Ramos, G. Cofré, R. Estévez, A. Salinas and J. Auger. 2011. Characterization of *Botrytis cinerea* Isolates Present in Thompson Seedless Table Grapes in the Central Valley of Chile. Plant Disease, 95: 683-90. https://doi.org/10.1094/pdis-04-10-0298

Fournier, E., T. Giraud, C. Albertini and Y. Brygoo. 2005. Partition of the *Botrytis cinerea* complex in France using multiple gene genealogies. Mycologia, 97: 1251-67. https://doi.org/10.3852/mycologia.97.6.1251

Fournier, E., T. Giraud, A. Loiseau, D. Vautrin, A. Estoup, M. Solignac, J. M. Cornuet and Y. Brygoo. 2002. Characterization of nine polymorphic microsatellite loci in the fungus *Botrytis cinerea* (Ascomycota). Molecular Ecology Notes, 2: 253-55. https://doi.org/10.1046/j.1471-8286.2002.00207.x

Fournier, E., C. Levis, D. Fortini, P. Leroux, T. Giraud and Y. Brygoo. 2003. Characterization of Bc-hch, the *Botrytis cinerea* Homolog of the Neurospora

crassa het-c Vegetative Incompatibility Locus, and Its Use as a Population Marker. Mycologia, 95: 251. https://doi.org/10.2307/3762036

Giraud, T., D. Fortini, C. Levis, C. Lamarque, P. Leroux, K. LoBuglio and Y. Brygoo. 1999. Two Sibling Species of the *Botrytis cinerea* Complex,transposaandvacuma, Are Found in Sympatry on Numerous Host Plants. Phytopathology, 89: 967-73. https://doi.org/10.1094/phyto.1999.89.10.967

Giraud, T., D. Fortini, C. Levis, P. Leroux and Y. Brygoo. 1997. RFLP markers show genetic recombination in *Botryotinia fuckeliana* (*Botrytis cinerea*) and transposable elements reveal two sympatric species. Molecular Biology and Evolution, 14: 1177-85. https://doi.org/10.1093/oxfordjournals.molbev.a025727

Karakaya, A. and H. Bayraktar. 2009. Botrytis disease of kiwifruit in Turkey. Australasian Plant Disease Notes, 4: 87-88.

Kumari, S., P. Tayal, E. Sharma and R. Kapoor. 2014. Analyses of genetic and pathogenic variability among *Botrytis cinerea* isolates. Microbiological Research, 169: 862-72. https://doi.org/10.1016/j.micres.2014.02.012

Leroux, P., R. Fritz, D. l. Debieu, C. Albertini, C. Lanen, J. Bach, M. Gredt and F. Chapeland. 2002. Mechanisms of resistance to fungicides in field strains of *Botrytis cinerea*. Pest Management Science, 58: 876-88. https://doi.org/10.1002/ps.566

Leroux, P., M. Gredt, M. Leroch and A. S. Walker. 2010. Exploring Mechanisms of Resistance to Respiratory Inhibitors in Field Strains of *Botrytis cinerea*, the Causal Agent of Gray Mold. Applied and Environmental Microbiology, 76: 6615-30. https://doi.org/10.1128/aem.00931-10

Levis, C., D. Fortini and Y. Brygoo. 1997. Flipper, a mobile Fot1-like transposable element in *Botrytis cinerea*. Molecular and General Genetics MGG, 254: 674-80. https://doi.org/10.1007/s004380050465

LÓPez-Berges, M. S., A. Di Pietro, M. J. Daboussi, H. A. Wahab, C. Vasnier, M. I. G. Roncero, M. Dufresne and C. Hera. 2009. Identification of virulence genes in Fusarium oxysporum f. sp. lycopersici by large-scale transposon tagging. Molecular Plant Pathology, 10: 95-107. https://doi.org/10.1111/j.1364-3703.2008.00512.x

Ma, Z. and T. J. Michailides. 2005. Genetic Structure of *Botrytis cinerea* Populations from Different Host Plants in California. Plant Disease, 89: 1083-89. https://doi.org/10.1094/pd-89-1083

Martinez, F., B. Dubos and M. Fermaud. 2005. The Role of Saprotrophy and Virulence in the Population Dynamics of *Botrytis cinerea* in Vineyards. Phytopathology, 95: 692-700. https://doi.org/10.1094/phyto-95-0692

Mirzaei, S., E. Mohammadi Goltapeh, M. Shams-Bakhsh, N. Safaie and M. Chaichi. 2009. Genetic and Phenotypic Diversity among *Botrytis cinerea* Isolates in Iran. Journal of Phytopathology, 157: 474-82. https://doi.org/10.1111/j.1439-0434.2008.01518.x

Möller, E. M., G. Bahnweg, H. Sandermann and H. H. Geiger. 1992. A simple and efficient protocol for isolation of high molecular weight DNA from filamentous fungi, fruit bodies, and infected plant tissues. Nucleic Acids Research, 20: 6115-16. https://doi.org/10.1093/nar/20.22.6115

Moyano, C., C. Alfonso, J. Gallego, R. Raposo and P. Melgarejo. 2003. Comparison of RAPD and AFLP marker analysis as a means to study the genetic structure of *Botrytis cinerea* populations. European Journal of Plant Pathology, 109: 515-22. https://doi.org/10.1023/a:1024211112831

Muñoz, C., S. Gómez Talquenca, E. Oriolani and M. Combina. 2010. Genetic characterization of grapevine-infecting *Botrytis cinerea* isolates from Argentina. Revista Iberoamericana de Micología, 27: 66-70. https://doi.org/10.1016/j.riam.2009.12.006

Pande, S., M. Sharma, G. K. Kishore, L. Shivram and U. N. Mangala. 2010. Characterization of Botrytis cinerea isolates from chickpea: DNA polymorphisms, cultural, morphological and virulence characteristics. African Journal of Biotechnology, 9: 7961-67.

Rigotti, S. 2002. Characterization of molecular markers for specific and sensitive detection of *Botrytis cinerea* Pers.: Fr. in strawberry (Fragaria×ananassa Duch.) using PCR. FEMS

Microbiology Letters, 209: 169-74. https://doi.org/10.1016/s0378-1097(02)00491-3

Rodríguez, H., L. Aguilar and M. LaO. 1997. Variations in xanthan production by antibiotic-resistant mutants of *Xanthomonas campestris*. Applied Microbiology and Biotechnology, 48: 626-29. https://doi.org/10.1007/s002530051106

Samuel, S., T. Veloukas, A. Papavasileiou and G. S. Karaoglanidis. 2012. Differences in Frequency of Transposable Elements Presence in *Botrytis cinerea* Populations from Several Hosts in Greece. Plant Disease, 96: 1286-90. https://doi.org/10.1094/pdis-01-12-0103-re

Schilling, J., J. Vivekananda, M. A. Khan and N. Pandey. 2013. Vulnerability to environmental risks and effects on community resilience in mid-west Nepal and south-east Pakistan. Environment and Natural Resources Research, 3: 27.

Shirane, N. 1989. Light Microscopic Observation of Nuclei and Mitotic Chromosomes of Botrytis Species. Phytopathology, 79: 728. https://doi.org/10.1094/phyto-79-728

Staats, M. 2004. Molecular Phylogeny of the Plant Pathogenic Genus Botrytis and the Evolution of Host Specificity. Molecular Biology and Evolution, 22: 333-46. https://doi.org/10.1093/molbev/msi020

Tamura, K., G. Stecher, D. Peterson, A. Filipski and S. Kumar. 2013. MEGA6: Molecular Evolutionary Genetics Analysis Version 6.0. Molecular Biology and Evolution, 30: 2725-29. https://doi.org/10.1093/molbev/mst197

Tanovic, B., G. Delibasic, J. Milivojevic and M. Nikolic. 2009. Characterization of *Botrytis cinerea* isolates from small fruits and grapevine in Serbia. Archives of Biological Sciences, 61: 419-29. https://doi.org/10.2298/abs0903419t

Wahab, H. A., M. Aboelghar, M. S. Moustafa and A. M. Ali. 2019. Hyperspectral analysis of *Botrytis cinerea* infected lettuce. EPH-International Journal of Agriculture and Environmental Research, 5: 26-42.

White, T. J., T. Bruns, S. Lee and J. Taylor. 1990. Amplification and direct sequencing of fungal ribosomal RNA genes for phylogenetics PCR protocols PCR Protocols. Elsevier. pp. 315-22.